Biomed Microdevices (2012) 14:1069–1076
DOI 10.1007/s10544-012-9698-8

Inkjet printing of protein microarrays on freestanding polymeric nanofilms for spatio-selective cell culture environment

Toshinori Fujie · Andrea Desii · Letizia Ventrelli · Barbara Mazzolai · Virgilio Mattoli

Published online: 18 September 2012

Abstract In the last years, an increasing interest in bio-hybrid systems for what concerns the precise control of cell-material interactions has emerged. This trend leads towards the development of new nano-structured devices such as bioMEMS, tissue-engineering scaffolds, biosensors, *etc*. In the present study, we focused on the development of a spatio-selective cell culture environment based on the inkjet printing of bio-patterns on polymeric ultra-thin films (nanofilms) composed of poly (methylmethacrylate) (PMMA). Freestanding PMMA nanofilms having hundreds-of-nm thickness were prepared by spin-coating. Different shapes of cell adhesion promoters such as poly (L-lysine) (PLL) were micropatterned by inkjet printing. Moreover, to promote cell adhesion, the surface of PLL microarrays was modified with fibronectin *via* electorostatic interaction. The selective deposition of C2C12 skeletal muscle cells was confirmed and their viability was qualitatively assessed after 24 h. The combination of muscular cells with protein micropatterned freestanding nanofilm is beneficial for the implementation of new bio-hybrid system in muscular tissue engineering.

Keywords Nanofilms · Skeletal muscle cells · C2C12 · Bio-hybrid devices · Inkjet printing

Andrea Desii and Toshinori Fujie contributed equally to this work.

T. Fujie · A. Desii (✉) · L. Ventrelli · B. Mazzolai · V. Mattoli
Center for MicroBioRobotics @SSSA, Istituto Italiano di Tecnologia,
Viale Rinaldo Piaggio, 34,
56025 Pontedera, PI, Italy
e-mail: andrea.desii@iit.it

T. Fujie
e-mail: fujie@wpi-aimr.tohoku.ac.jp

V. Mattoli
e-mail: virgilio.mattoli@iit.it

T. Fujie
European Biomedical Science Institute (EBSI), Organization for European Studies, Waseda University,
2-2 Wakamtsu-cho,
Shinjuku, Tokyo 162-8480, Japan

A. Desii · L. Ventrelli
The Biorobotics Institute, Scuola Superiore Sant'Anna, Polo Sant'Anna Valdera,
Viale Rinaldo Piaggio, 34,
56025 Pontedera, PI, Italy

T. Fujie
WPI-Advanced Institute for Materials Research,
Tohoku University,
2-1-1, Katahira,
Aoba-ku, Sendai 980-8577, Japan

1 Introduction

Recent developments in nanotechnology have led us to discover a method for producing a biocompatible freestanding polymeric ultra-thin film (nanofilm) (Fujie et al. 2007). Compared with bulk films, these polymeric nanofilms exhibited unique physical properties represented by high transparency, non-covalent adhesion and high flexibility, due to their huge surface-thickness aspect ratio (over 10^6, with a surface of tens of cm^2). These properties were utilized for biomedical applications as a new type of surgical device (e.g. wound dressing material) or cell culture platform (Fujie et al. 2009, 2010; Ricotti et al. 2010). In particular, development of polymeric nanofilms for the cell culture platform has been an active focus because of the wide-spread application in the field of tissue engineering, but also soft robotics utilizing contractive cells (Feinberg et al. 2007). There have been several attempts to produce micro-patterned protein arrays on a thin film interface, using methods such as photolithography (Mooney et al. 1996; Welle and Gottwald 2002), micro-contact printing (Kane et al. 1999), nano/micro-imprinting (Hoff et al. 2004) and electrochemical oxidation (Kaji et al. 2005). However, considering the process integration, these approaches were not

always adequate in order to produce large dimensional micro-patterned arrays conveniently and rapidly. In contrast, inkjet printing technology has been recently developed for high-throughput (macro)molecules patterning (Tekin et al. 2008; Singh et al. 2010).

Inkjet printing consists in the deposition over a planar surface of small liquid droplets ejected through a small orifice. Every fluid that satisfies specific viscosity and surface tension requirements can be printed, and indeed examples of deposition of nanoparticles dispersions (van Osch et al. 2008), functional polymer solutions (Bharathan and Yang 1998), cell suspension (Xu et al. 2005; Saunders et al. 2008) can be found in literature.

Piezoelectric drop-on-demand (DoD) inkjet printing technology is especially suitable for the patterned deposition of small droplets of biological solutions and suspensions (Delaney et al. 2009), due to the fact that cells and biomacromolecules are not able to withstand aggressive treatments typical of other microfabrication methods (organic solvents, UV light exposure, baking, etc.). Biologists and engineers tried successfully the inkjet printing of proteins (Sanjana and Fuller 2004; Roth et al. 2004; Zarowna-Dabrowska et al. 2012), biocompatible polymers (Kim et al. 2010; Yamazoe and Tanabe 2009) and nucleic acids (Goldmann and Gonzalez 2000; Bietsch et al. 2004).

The minimum resolution of this patterning method depends on the properties of the ejected liquid, but for most applications is not less than a few tens of μm (Calvert 2001). Although the thinnest lines achievable are tens of μm wide, cytophilic stripes for the anisotropic adhesion and alignment of living cells (typically tens of μm in diameter) could be obtained printing adhesion promoters such as poly(L-lysine) (PLL) and fibronectin (FN) on the entire surface of a polymeric thin film.

Precise alignment of protein and cell in micro-featured scale has been developed by surface modification of hot-embossed poly(carbonate) (Charest et al. 2007), soft lithographical micro-contact printing of protein arrays with poly(dimethylsiloxane) molds (Feinberg et al. 2007) or by tuning the surface chemistry of cytophobic/cytophilic substrates using synthetic polymer brushes (Fujie et al. 2011a). In all these studies, anisotropic skeletal muscle cell alignment and formation of myotubes was observed when feature size was not exceeding 100 μm, a feature size limit that can be reached using an inkjet printing method.

In this study, the micro-patterning of fibronectin on polymeric nanofilms by an inkjet printing process and spatio-selective culture of skeletal muscle cells on the printed nanofilms are reported. Moreover, the protein micro-patterned nanofilm was exfoliated from the substrate as a freestanding structure. Such substrates could be used as support layers in biohybrid actuators based on contractile cells and ubiquitously transferrable bioscaffolds in tissue engineering.

2 Materials and methods

2.1 Fabrication of freestanding PMMA nanofilms

Freestanding polymeric nanofilms able to withstand cell culture conditions without being released were obtained as follows (Fig. 1). SiO_2 wafers (Si-Mat Silicon Materials, Landsberg Am Lech, Germany) were cut in 2 cm×2 cm fragments, dipped in Nanostrip (Cyantek, Fremont, CA) for 20 min at 60 °C and then washed under running deionized water. A 100 mg ml^{-1} solution of poly(N-isopropylacrylamide) (PNIPAm) (Sigma-Aldrich, St. Louis, MO) in propan-2-ol was deposited on wafer fragments by spin-coating (4000 rpm, 60 s) to obtain a thermoresponsive sacrificial layer. The substrates were heated at 80 °C for 90 s to remove excess solvent. A tens-of-nm thick polymeric layer was prepared by spin-coating a 40 mg ml^{-1} solution of poly (methyl methacrylate) (PMMA) (Sigma-Aldrich) in toluene over the sacrificial layer and heated at 110 °C for 5 min to remove adsorbed toluene. Then, bovine serum albumin (BSA) (Sigma-Aldrich) was physically adsorbed on the PMMA surface before the deposition of a polycation solution by inkjet printing. 300 μL of a 10 μg ml^{-1} solution of BSA in 1 % dimethylsulfoxide (DMSO) was drop cast overnight on each nanofilm over a heating plate at 40 °C, and then rinsed three times with deionized water at 40 °C to avoid the dissolution of sacrificial layer. The samples were dried on a heating plate at 40 °C before starting the printing process.

Film thickness was evaluated on nanofilms collected on SiO_2 wafers after water release. Briefly, the nanofilm surface was scratched and thickness profiles over 500 μm distance in lateral direction across the scratch were recorded using a P-6 profilometer (KLA-Tencor, Milpitas, CA).

2.2 Inkjet printing of PLL microarrays on PMMA nanofilms

Deposition of fluoresceine isothiocyanate modified poly(L-lysine) (FITC-PLL) (Sigma-Aldrich) was performed using a DMP-2800 piezoelectric drop-on-demand inkjet materials printer (Fujifilm DIMATIX, Santa Clara, CA). A 10 pL droplet ink cartridge was filled with 1.5 ml of a 1 mg ml^{-1} FITC-PLL water solution. The substrate platen was heated at 37 °C during the printing process to increase the ink evaporation rate in order to avoid blotting due to excessive droplet merging. Ink was ejected through a single nozzle to obtain more reproducible results.

Patterns were designed using a vector graphics software, Inkscape (http://inkscape.org), then exported in bitmap format to be loaded by the printer software. Horizontal parallel lines with width ranging from 25 μm to 500 μm, concentric rings 100 μm wide with increasing radii, microgrids were among the patterns prepared to be printed. Color space for

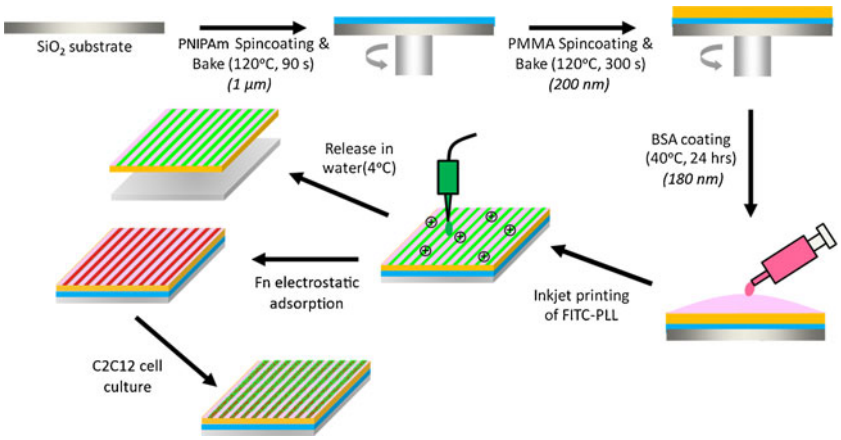

Fig. 1 Fabrication scheme of freestanding inkjet-patterned nanofilm. Film thickness for each layer is reported in italics

all images was binary, with black pixels corresponding to single ejection events.

Printed substrates were observed with a T*i*-E inverted epifluorescent microscope (Nikon Instruments, Tokio, Japan) equipped with fluoresceine and rhodamine filters and a DS-5MC cooled CCD camera (Nikon Instruments). Digital images were collected using NIS Elements imaging software (Nikon Instruments) and elaborated with ImageJ (http://rsbweb.nih.gov/ij/) and Igor Pro (WaveMetrics, Lake Oswego, OR) image processing and analysis software. To perform line width measurement, images were imported in Igor Pro where 8-bit RGB FITC filtered images were converted in grayscale and isolated from the darker background by thresholding. The binary thresholded images were averaged along the direction perpendicular to lines direction, and line width was evaluated as the half-height width of the color value average profile.

Printed substrates were washed three times with warm phosphate buffered saline at pH 7.4 (PBS) and then transferred to fibronectin solution in PBS for protein adsorption experiments.

2.3 Skeletal muscle cell culture and seeding

Fibronectin (FN) (Sigma-Aldrich) was labeled with tetramethylrhodamine isothiocyanate (TRITC) (Sigma-Aldrich) using a method adapted from Larsson (1988). 12 μL of a 1 mg ml^{-1} TRITC solution in dimethylsulfoxide were added to 2 mL of a 1 mg ml^{-1} FN solution in carbonate/bicarbonate buffer at pH 9.0. The solution was incubated for 2 h in the dark, and then unbound TRITC was removed by filtration with a 10000 MWCO Amicon Ultra-4 centrifugal filter unit (EMD Millipore, Billerica, MA). FN carbonate buffer was replaced with PBS by spin filtration. The resulting 1 mg ml^{-1} solution (TRITC-FN) was diluted to 10 μg ml^{-1} and separated in single use aliquots. Printed substrates were incubated in diluted FN solution for 2 h at 37 °C, washed thoroughly using warm PBS and transferred to fresh medium for microscope imaging.

C2C12 mouse myoblasts (CRL-1772, ATCC, Manassas, VA) were cultured in Dulbecco's modified Eagle's medium (DMEM) (ATCC) supplemented with 10 % fetal bovine serum (FBS) (ATCC), 100 IU ml^{-1} penicillin, 100 μg ml^{-1} streptomycin and 2 mM L-glutamine. Cells were maintained in normal culture conditions (37 °C, saturated humidity atmosphere at 95 % air/5 % CO_2) and subcultured onto T25 flasks before reaching 60–70 % confluence. Cells were detached from the flasks using a 0.05 wt.% trypsin with phenol red solution. The aliquot was subsequently purified by centrifugation and suspended in fresh culture medium. Prior to C2C12 seeding, the patterned nanofilms (4 cm^2) were placed in sterile Petri dishes and then sterilized by UV irradiation for 30 min. After sterilization, the samples were washed three times with PBS at 37 °C and moved in a 6-wells cell culture plate. Finally, 2 ml of cell suspension (2.5×10^4 cells ml^{-1}) were used to cover each well containing the PMMA nanofilm, and incubated in the cell incubator for 30 min to allow cells attachment on the nanofilms surface. Additional culture medium was then added to the wells, and the samples were cultured under standard conditions for 24 h.

2.4 Cytocompatibility assay

C2C12 cells vitality on PMMA nanofilms was qualitatively investigated at 24 h after cell seeding using the LIVE/DEAD® Viability/Cytotoxicity Kit (Invitrogen Co.). The kit contains calcein AM (4 mM in anhydrous DMSO) and ethidium homodimer-1 (EthD-1, 2 mM in DMSO/H_2O 1:4 v/v), and it identifies live versus dead cells on the basis of membrane integrity and esterase activity. Cells were incubated for 24 h at standard culture conditions, then the culture medium was removed and the cellular layers onto the samples surface were rinsed with PBS and treated for 10 min at 37 °C with 2 μM calcein AM and 4 μM EthD-1. Cells were finally observed with the T*i*-E inverted fluorescent microscope. Live cells percentage was evaluated as the average ratio between live cells and total stained cells on each line

(dead+live cells). Cell counting was performed using the cell counter plugin of ImageJ.

3 Results and discussions

3.1 Characterization of freestanding PMMA nanofilms

It was recently demonstrated that free-standing ultra-thin films can serve as cell culture substrates for skeletal muscle cells (Ricotti et al. 2010). Cells adhered to the freestanding surface homogeneously, on both sides. This has to be avoided for a patterned cell culture substrate, because cells need to adhere only on the upper, modified surface. To achieve specific adhesion, ultra-thin films should be released from their supporting material (glass, SiO_2) only after cell seeding and proliferation, therefore a sacrificial layer not soluble in cell culture medium condition is needed. Moreover, the rigidity of the underlying SiO_2 substrate improves cell adhesion and proliferation on the surface of the softer polymeric material, as demonstrated for nanofilms supported on metal grids (Fujie et al. 2011b). PNIPAm exhibits a lower critical solution temperature (LCST) in water at 32 °C, lower than cell incubation temperature (37 °C): this means that a PNIPAm sacrificial layer is stable during incubation and can be dissolved simply by putting it at 4 °C in a refrigerator for a few minutes.

PNIPAm solutions in propan-2-ol were spin deposited on SiO_2 surfaces to obtain thermo-responsive sacrificial layers. PMMA thin-films can be deposited on top of the sacrificial layer from a PMMA solution in toluene, an orthogonal solvent for PNIPAm. By cutting the edges of the film and submerging it in cold water (4 °C), a free-standing PMMA ultra-thin film was released from the SiO_2 wafer in a few minutes and floated to the water-air interface to minimize the interfacial energy of the hydrophobic polymeric film. In water at 20 °C the same process occurred during a longer period, up to a few hours. Above the LCST, the film was stable on top of the wafer surface.

The high flexibility of ultra-thin polymer films (Okamura et al. 2009) provides an ideal support for contractile cells. The contraction is impaired by rigid substrates (Feinberg et al. 2007) and more generally, if cells spend energy to deform their support, less mechanical energy would be available for the displacement of the biohybrid device. In this framework, the objective is to reduce the thickness of the cell supporting film to a value sufficient to guarantee high flexibility and stability under mechanical stress. Mechanical characterization of poly(lactic acid) (PLA) films confirms that submicrometer flexible polymer membranes can withstand the mechanical stresses due to cell contraction (Ricotti et al. 2010). It could be easily assumed that an ultra thin film of PMMA could have the same general behavior, with the important difference that its precursor polymer is soluble in an orthogonal solvent for PNIPAm, which is not the case for PLA membranes. Moreover, PMMA is stable under physiological conditions and its mechanical properties do not change under prolonged exposure to cell culture media, providing a reliable substrate for biohybrid actuation applications. PMMA films were 199±20 nm thick, a value compatible with all these mechanical requirements. Therefore, by using cell scaffolds based on thermally releasable ultra-thin films, the rigidity of the surface can be controlled: the stiffer supported film improves cell adhesion and proliferation during culture, while the soft, flexible support obtained after release could be ideal for contractile cells energy harvesting.

Albumin modified surfaces have been shown to be protein repellant. Cell adhesion to a solid surface is mediated by membrane proteins, therefore effective protein repulsion by a surface leads to effective cell repulsion (Kragh-Hansen 1981). To achieve spatial control on cell adhesion and proliferation, a surface has to carry cytophobic and cytophilic moieties.

The PMMA thin film was modified with BSA to obtain a cytophobic background over which a cytoadhesive molecule could be patterned. Stable adsorption of albumin on PMMA surfaces was already demonstrated in several

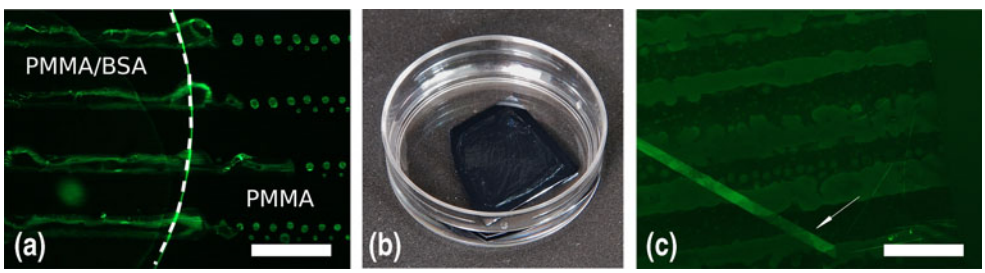

Fig. 2 FITC-PLL printed nanofilm. (**a**) FITC fluorescence image of ink adsorption on BSA covered substrate and ink dewetting on PMMA uncoated surface. (**b**) Free-standing nanofilm floating in water over its supporting wafer in a 35 mm Petri dish. (**c**) Fluorescence image of a printed nanofilm collected on a glass slide from the release medium. Notably, the film folded without breaking (the wrinkle is indicated by the arrow). All scale bars 500 μm

studies (Suzawa and Murakami 1980; Cheng et al. 1987), as well as adsorption on free-standing ultra-thin membranes (Ozaydin Ince et al. 2010). BSA was drop cast on the film from a water solution containing 1 % of a high boiling point solvent (DMSO) to avoid coffee ring effects and other evaporation defects (Deegan et al. 1997; Lim et al. 2008). Solvent evaporation was performed at 40 °C to avoid excessive swelling of the PNIPAm caused by the eventual permeation of the solvent through defects in the ultra-thin PMMA membrane, which could result in rips in the polymer film by an increase of the mechanical tension. Non adsorbed BSA was removed washing the surface three times with warm water. The BSA layer thickness of 180±50 nm excludes the hypothesis of immobilization of albumin on the PMMA surface by physical adsorption only. Therefore, there is a large quantity of reversibly immobilized BSA, but the dissolution of the drop cast layer is slow enough to allow cell culturing and all manipulation processes of the nanofilm in liquid solutions, while preserving surface functionality for 24 h. An alternative BSA immobilization strategy will be evaluated if the stability of the surface will be insufficient for cell processes requiring longer culture times, such as proliferation studies and differentiation.

3.2 Inkjet-printed PLL microarrays

At pH 7.4 albumin surface is negatively charged. Polycations can therefore be adsorbed irreversibly on an albumin modified surface (Mattison et al. 1998), i.e., a small droplet of a PLL solution leaves an electrostatically adsorbed polycation layer on an albumin modified surface upon evaporation of the solvent. The inkjet printing technique is based on the sequential, programmed deposition of small droplet of fluids on planar surfaces. To confirm the printability of PLL solutions, printing tests employing fluorescein isothiocyanate labeled PLL (FITC-PLL) were performed, in order to characterize the output using an epifluorescent microscope.

FITC-PLL was effectively adsorbed on the BSA surface, while it formed small clusters on the uncoated PMMA surface upon evaporation of the solvent, resulting in dotted, discontinuous patterns (Fig. 2(a)). The resulting film could be easily suspended in water upon dissolution of the PNIPAm sacrificial layer. In contrast to PMMA uncoated nanofilms, the samples floated inside the release medium without spreading on the liquid-air interface, due to the hydrophilic BSA/PLL side (Fig. 2(b)). It was possible to reproduce rectilinear and curvilinear patterns with features as small as 80 μm (Fig. 3(a)–(b)). Even more complicated patterns were easy to obtain (Fig. 3(c)). It is worth noting that printing the FITC-PLL ink required minimal optimization of the solution properties and ejection parameters, allowing

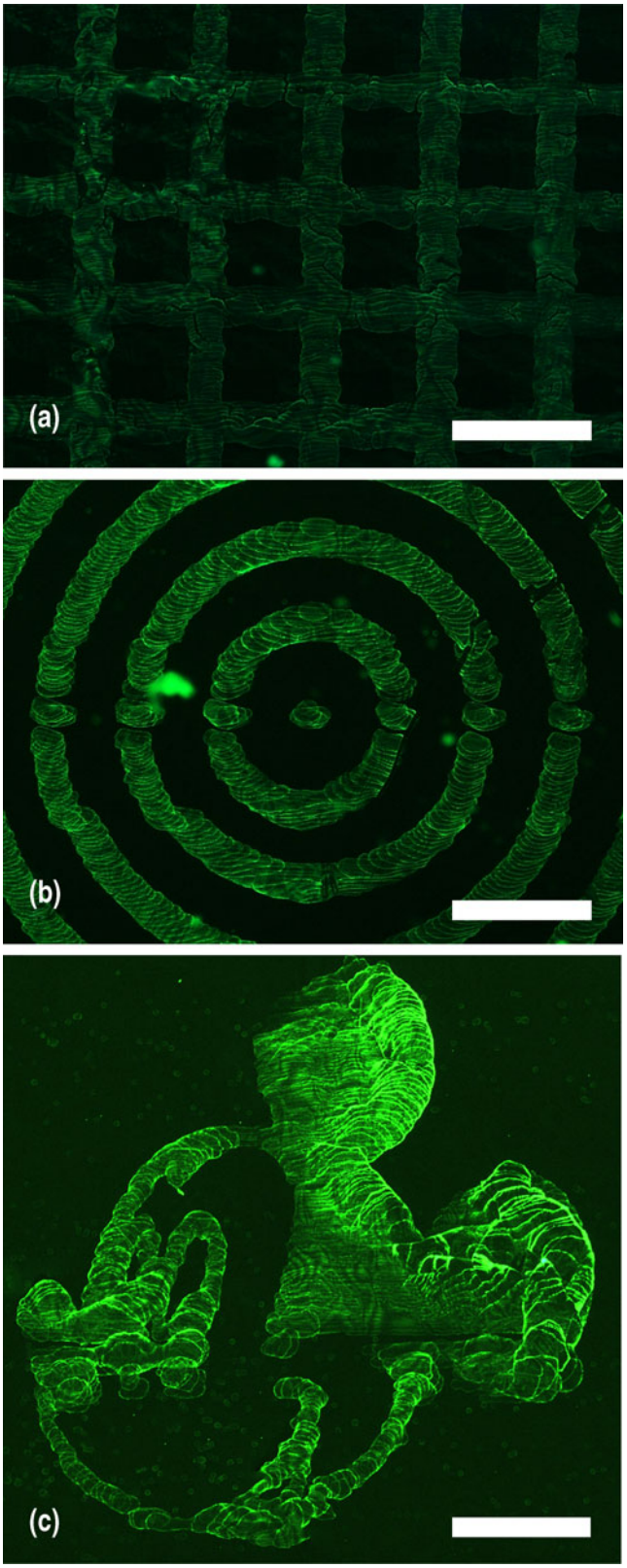

Fig. 3 Inkjet printed FITC-PLL patterns on BSA covered PMMA nanofilm. (**a**) Grid of lines (100 μm wide) separated by 300 μm. (**b**) Concentric circles of 100 μm wide lines with increasing diameter. (c) Printed Mickey Mouse (© The Walt Disney Company). All scale bars 500 μm

for fast and easy design and implementation of custom patterns. A calibration array of parallel lines was designed to better characterize the relation between input pattern dimensions and output feature size (Fig. 4 (a)–(c)). Output/Input line width ratio decreased with increasing width, highlighting the limit represented by the minimum droplet impression size. On hydrophilic substrates water droplets tend to spread and their border is pinned to the surface during evaporation, effectively limiting the reduction in feature size. The limit could be partially overcome by using cartridges with smaller nozzle size which can eject smaller volume droplets. Standard deviation for small line width is relatively larger due to the increased importance of defects at small scales (Fig. 4(d)).

The immobilization of FITC-PLL on the surface after washings and film release was confirmed by imagining a released film recollected on a glass slide and air dried (Fig. 2(c)). The irreversible adsorption of FITC-PLL on the BSA substrate testifies their stabilization by electrostatic interaction.

3.3 Selective deposition of C2C12 cells on the micropatterned nanofilm

PLL/FN electrostatic association has been widely demonstrated in literature (Wittmer et al. 2007), while albumin covered surfaces have been shown to be protein repellent. Fibronectin immobilization on FITC-PLL was tested employing TRITC-FN. Specific adsorption of TRITC-FN was confirmed by epifluorescent microscopy. Rhodamine fluorescence images can be perfectly superimposed on analogous fluorescein images (Fig. 5(a)–(c)). It is of the utmost importance to use freshly purified TRITC-FN during the association step, otherwise unbound TRITC could be adsorbed by the hydrophobic albumin surface, hindering the visualization of associated FN.

Selective cell adhesion on TRITC-FN patterns was observed after 24 h (Fig. 6(a)). Live cells attached to the nanofilm surface were green stained, while red denotes cells that underwent apoptosis. Cells attached outside the intended print pattern were due to print defects, not to unspecific adhesion. This is confirmed in Fig. 6(b), where the exposition time for red fluorescence was longer than in Fig. 6(a): fluorescence due to TRITC-FN and apoptotic cells was simultaneously collected. The percentage of live cells over total attached cells evaluated on each printed line is 96.1±2.1 %. Apoptotic cells are the bright yellow spots, while TRITC-FN adsorbed on PLL satellite droplets outside the intended pattern are visualized as darker spots. Live cells in Fig. 6(a) can be observed in correspondence of darker red spots in Fig. 6(b). The test confirmed the selective adsorption of the C2C12 cells and the cytocompatibility of the nanofilms. Our methodology of inkjet printing process will be beneficial for the application as biorobotics systems in combination with contractile muscular cells. Compared to similar methods

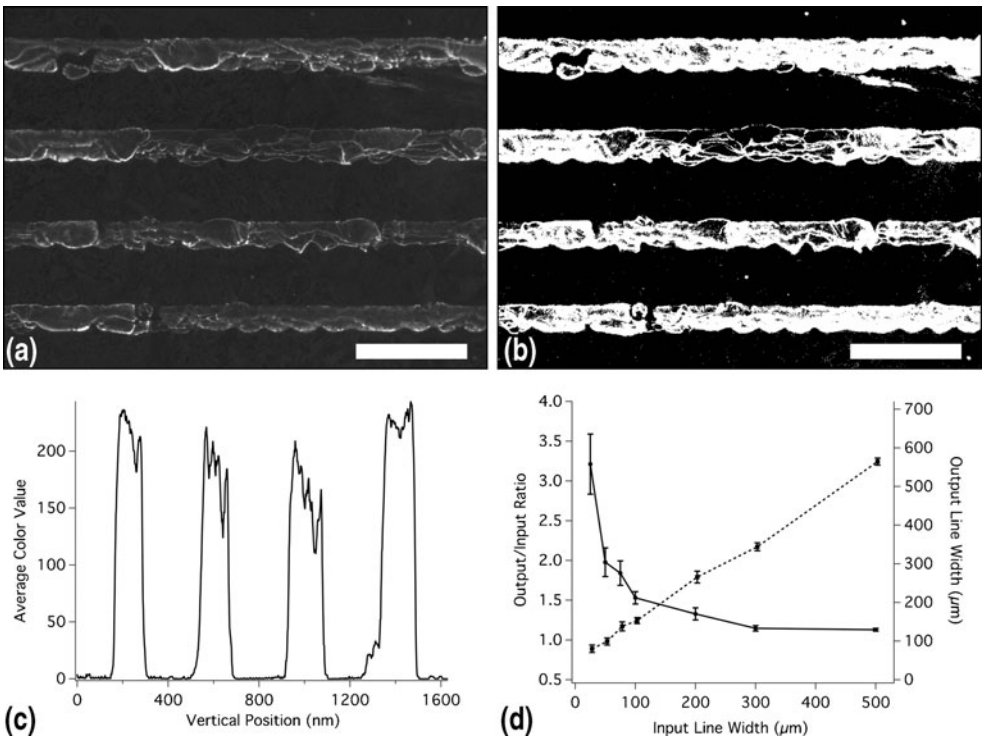

Fig. 4 Line width measurement and Output/Input characterization. (**a**) Grayscale FITC fluorescence image of FITC-PLL lines with input width of 100 μm (*top two*) and 75 μm (*bottom two*). (**b**) Image binarization of (**a**). (**c**) Average vertical profile of (**b**). (**d**) Variation of output line width (■, dotted) and output/input ratio (●, solid) with input line width. All scale bars 500 μm

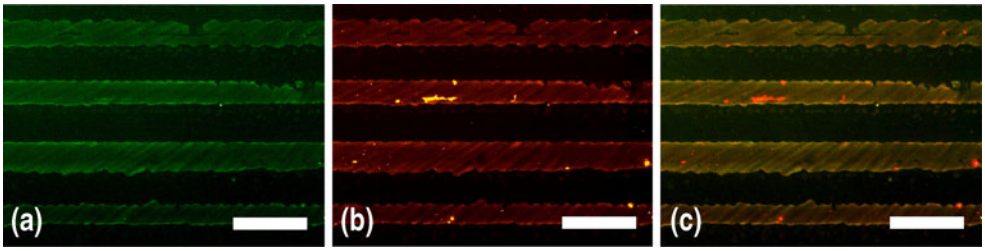

Fig. 5 Fluorescence microscopy of TRITC-FN adsorbed on printed FITC-PLL. (**a**) FITC fluorescence image of 150 μm wide lines array. (**b**) TRITC fluorescence image of the same area. (**c**) Superposition of (**a**) and (**b**). All scale bars 500 μm

employing soft lithography of proteins on PDMS thin membranes, our strategy allows a higher throughput and is independent from the absorption of the protein solution inside the stamp. Moreover, thinner, more conformable films are achievable. Electrostatic association of biomacromolecules offers a versatile platform for further modification and for the implementation of multifunctional devices. Furthermore, micropatterned cell substrates on freestanding nanofilms will be applicable as implantable biodevices in regenerative medicine.

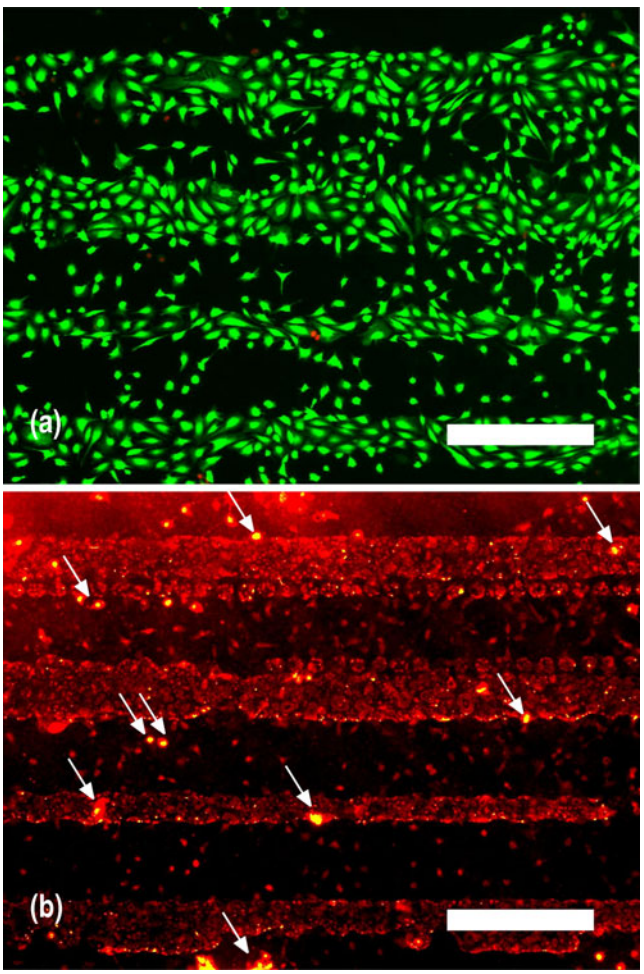

Fig. 6 LIVE/DEAD cell viability and cytotoxicity assay. (**a**) Superposition of FITC fluorescence and TRITC fluorescence images of C2C12 cells cultured on printed nanofilms (input width: 150 μm top two lines, 75 μm bottom two lines). Live cells are green, while dead cells are red stained. Exposure time 80 ms (**b**) TRITC fluorescence image evidencing dead cells (bright yellow spots indicated by arrows) and TRITC-FN fluorescence. Exposure time 1 s. All scale bars 500 μm

4 Conclusions

In the framework of the development of hybrid top-down/bottom-up fabrication processes, the combination of inkjet printing and electrostatic protein adsorption can represent a versatile and high-throughput methodology to develop microstructured biomedical devices. Such approach allows the production of freestanding and flexible protein microarrays exploitable as spatioselective cell culture platforms. Inkjet printing is a fast and reliable micropatterning method for the modification of polymeric nanofilms with cell adhesive biomacromolecules (i.e., PLL). Electrostatic adsorption was exploited to associate PLL to BSA and subsequently FN to PLL, in order to obtain a surface with alternating cytophobic/cytophilic moieties, on which cells from the C2C12 line were successfully patterned and cultured. On the other hand, a protocol to obtain freestanding nanofilms that can be released after cell seeding and proliferation was developed. The resulting biodevice combines the advantages of a rigid, supported and patterned cell culture environment (possibility to control attachment side, improved cell adhesion) with the flexibility required for high substrate conformability. These properties suggest a possible application of this technology as conformable patterned cell scaffolds in tissue engineering or as flexible supports for biohybrid robotic devices based on aligned contractile muscular cells. Moreover, a PLL patterned surface is susceptible to further modification with different negatively charged macromolecules or nanoparticles, representing a microstructured template to produce biomedical microdevices.

Future work will involve the study of cell differentiation and myotube formation, the reduction of printed feature size by process optimization and the implementation of different modification to introduce other functionalities.

References

J. Bharathan, Y. Yang, Appl. Phys. Lett. **72**(21), 2660 (1998)

A. Bietsch, M. Hegner, H.P. Lang, C. Gerber, Langmuir **20**(12), 5119 (2004)

P. Calvert, Chem. Mater. **13**(10), 3299 (2001)

J.L. Charest, A.J. Garcia, W.P. King, Biomaterials **28**(13), 2202 (2007)

Y.L. Cheng, S.A. Darst, C.R. Robertson, J. Colloid Interf. Sci. **118**(1), 212 (1987)

J.T. Delaney, P.J. Smith, U.S. Schubert, Soft Matter **5**(24), 4866 (2009)

R.D. Deegan, O. Bakajin, T.F. Dupont, G. Huber, S.R. Nagel, T.A. Witten, Nature **389**(23), 827 (1997)

A.W. Feinberg, A. Feigel, S.S. Shevkoplyas, S. Sheehy, G.M. Whitesides, K.K. Parker, Science **317**(5843), 1366 (2007)

T. Fujie, Y. Okamura, S. Takeoka, Adv. Mater. **19**(21), 3549 (2007)

T. Fujie, N. Matsutani, M. Kinoshita, Y. Okamura, A. Saito, S. Takeoka, Adv. Funct. Mater. **19**(16), 2560 (2009)

T. Fujie, S. Furutate, D. Niwa, S. Takeoka, Soft Matter **6**(19), 4672 (2010)

T. Fujie, H. Haniuda, S. Takeoka, J. Mater. Chem. **21**(25), 9112 (2011a)

T. Fujie, L. Ricotti, A. Desii, A. Menciassi, P. Dario, V. Mattoli, Langmuir **27**(21), 13173 (2011b)

T. Goldmann, J.S. Gonzalez, J. Biochem. Biophys. Meth. **42**(3), 105 (2000)

J.D. Hoff, L.J. Cheng, E. Meyhofer, L.J. Guo, A.J. Hunt, Nano Letters **4**(5), 853 (2004)

H. Kaji, K. Tsukidate, M. Hashimoto, T. Matsue, M. Nishizawa, Langmuir **21**(15), 6966 (2005)

R.S. Kane, S. Takayama, E. Ostuni, D.E. Ingber, G.M. Whitesides, Biomaterials **20**(23–24), 2363 (1999)

J.D. Kim, J.S. Choi, B.S. Kim, Y.C. Choi, Y.W. Cho, Polymer **51**(10), 2147 (2010)

U. Kragh-Hansen, Pharmacol. Rev. **33**(1), 17 (1981)

L. Larsson, *Immunocytochemistry: Theory and Practice* (CRC, Boca Raton, 1988), pp. 224–225

J.A. Lim, W.H. Lee, H.S. Lee, J.H. Lee, Y.D. Park, K. Cho, Adv. Funct. Mater. **18**(2), 229 (2008)

K.W. Mattison, P.L. Dubin, I.J. Brittain, J. Phys. Chem. B **102**(19), 3830 (1998)

J.F. Mooney, A.J. Hunt, J.R. McIntosh, C.A. Liberko, D.M. Walba, C.T. Rogers, Proc. Natl. Acad. Sci. U. S. A. **93**(22), 12287 (1996)

Y. Okamura, K. Kabata, M. Kinoshita, D. Saitoh, S. Takeoka, Adv. Mater. **21**(43), 4388 (2009)

G. Ozaydin Ince, G. Demirel, K.K. Gleason, M.C. Demirel, Soft Matter **6**(8), 1635 (2010)

L. Ricotti, S. Taccola, V. Pensabene, V. Mattoli, T. Fujie, S. Takeoka, A. Menciassi, P. Dario, Biomedical Microdevices **12**(5), 809 (2010)

E.A. Roth, T. Xu, M. Das, C. Gregory, J.J. Hickman, T. Boland, Biomaterials **25**(17), 3707 (2004)

N.E. Sanjana, S.B. Fuller, J. Neurosci. Meth. **136**(2), 151 (2004)

R.E. Saunders, J.E. Gough, B. Derby, Biomaterials **29**(2), 193 (2008)

M. Singh, H.M. Haverinen, P. Dhagat, G.E. Jabbour, Adv. Mater. **22**(6), 673 (2010)

T. Suzawa, T. Murakami, J. Colloid Interface Sci. **78**(1), 266 (1980)

E. Tekin, P.J. Smith, U.S. Schubert, Soft Matter **4**(4), 703 (2008)

T.H.J. van Osch, J. Perelaer, A.W.M. de Laat, U.S. Schubert, Adv. Mater. **20**(2), 343 (2008)

A. Welle, E. Gottwald, Biomedical Microdevices **4**(1), 33 (2002)

C.R. Wittmer, J.A. Phelps, W.M. Saltzman, P.R. Van Tassel, Biomaterials **28**(5), 851 (2007)

T. Xu, J. Jin, C. Gregory, J.J. Hickman, T. Boland, Biomaterials **26**(1), 93 (2005)

H. Yamazoe, T. Tanabe, J Biomed Mater Res **91A**(4), 1202 (2009)

A. Zarowna-Dabrowska, E.O. McKenna, M.E. Schutte, A. Glidle, L. Chen, C. Cuestas-Ayllon, D. Marshall, A. Pitt, M.D. Dawson, E. Gu, J.M. Cooper, H.B. Yin, Colloids and Surfaces B-Biointerfaces **89**, 126 (2012)